Available online at www.sciencedirect.com
SCIENCE DIRECT
Polymer 46 (2005) 5065–5074
polymer
www.elsevier.com/locate/polymer

The disorderly exfoliated LDHs/PMMA nanocomposite synthesized by in situ bulk polymerization

Guo-An Wang[a], Cheng-Chien Wang[b], Chuh-Yung Chen[a,*]

[a]Department of Chemical Engineering, National Cheng-Kung University, Tainan 70101, Taiwan, ROC
[b]Department of Chemical Engineering, Southern Taiwan University of Technology, Tainan 710, Taiwan, ROC

Received 25 March 2005; received in revised form 26 April 2005; accepted 26 April 2005

Abstract

A new nanocomposite—disorderly exfoliated layered double hydroxides/poly(methyl methacrylate) (LDHs/PMMA)—was prepared by a two-stage process with an in situ bulk polymerization of methyl methacrylate (MMA) in the presence of 10-undecenoate intercalated LDH (LDH-U). The LDH-U was prepared using the co-precipitation method. The structural and compositional details of the LDH-U were determined by X-ray diffraction (XRD), Fourier transformed infrared spectroscopy (FT-IR), ^{27}Al and ^{13}C magic-angle spinning nuclear magnetic resonance (^{27}Al and ^{13}C MAS NMR), elemental analysis (EA), inductively coupled plasma-mass (ICP) and transmission electron microscopy (TEM). During the preparation of LDHs/PMMA nanocomposite, XRD and TEM were also employed to monitor the formation of the exfoliated LDHs/PMMA nanocomposite and the dispersion behavior of the LDH layers, respectively. The pre-polymerization process exfoliates LDH layers within pre-polymer, according to the XRD and TEM results. Additionally, the LDHs/PMMA nanocomposite contained 5 wt% LDH-U, indicating that the LDH layers were well exfoliated and dispersed in the PMMA matrix in a disordered fashion.

Keywords: Nanocomposites; Poly(methyl methacrylate); Layered double hydroxides

1. Introduction

The inorganic/polymer nanocomposites have attracted much attention for many years. Most studies of nanocomposites, over the last few years, have involved clays as an inorganic reinforcing material because clays have a large aspect ratio and considerable ion exchange capacity [1–3]. The structures of clay/polymer nanocomposites can be separated into two groups—intercalated and exfoliated [4,5]. Intercalated nanocomposites have polymer chains that penetrate into the interlayer gallery, and the distance of the layer is increased without completely separating the layers. Exfoliated nanocomposites are defined as having insufficient attractions between each two-layer section, which is the reason why these materials cannot maintain a uniform layer space. However, only a few stacks of clay layers, which are dispersed homogeneously in the polymer matrix, belong to the family of exfoliated nanocomposites. More commonly, the homogeneous dispersion of clay layers and the large interfacial area between polymer and clay make exfoliated clay/polymer nanocomposites desirable for greatly improving properties. Therefore, most previous investigations on clays have focused on montmorillonite-type layered silicate because its layers have a relatively low charge density and exfoliated layered silicate/polymer nanocomposites can be easily obtained. However, the variability of the composition, the charge density and the iron content of these naturally occurred montmorillonite-type layered clays significantly impedes the control of the properties of exfoliated clay/polymer nanocomposites properties. Accordingly, in this study, synthetic clay with layered double hydroxides (LDHs) is used as an inorganic material in preparing the clay/polymer nanocomposites.

The LDHs' structures consist of brucite-like sheets, in which divalent cations are partially replaced by trivalent cations, and interlayer anions compensate for the positively charged layers. The LDHs—the so-called anionic clays—can intercalate various anions in its interlayers. This intercalation determines the anion-exchange properties. The general formula for these materials is

* Corresponding author. Tel.: +886 6 2360468; fax: +886 6 2344496.
E-mail address: ccy7@ccmail.ncku.edu.tw (C.-Y. Chen).

0032-3861/$ - see front matter © 2005 Elsevier Ltd. All rights reserved.
doi:10.1016/j.polymer.2005.04.054

$(M^{2+}_{1-x}M^{3+}_{x}(OH)_2)^{x+}(A^{n-})_{x/n}\cdot mH_2O$, where M^{2+} and M^{3+} are the individual divalent and trivalent cations in octahedral sites within the OH-layers. A^{n-} is an exchangeable anion such as NO_3^- and SO_4^{2-} [6]. The anions are typically intercalated into LDHs' interlayers by the three experimental approaches—(1) the co-precipitation method, which requires the addition of an M^{2+}/M^{3+} metal salt solution to a base solution of the desired anions [7,8] (2) the direct ion exchange method, in which LDHs are stirred in a solution of desired anions at an suitably concentration [9], and (3) the rehydration method, in which calcined LDH is added to the solution of the desired anions [10].

The gallery distance between each pair of pristine LDH layers, such as hydrotalcite, is only approximately 2.97 Å, which is too narrow to allow monomer or polymer molecules to intercalate [6]. Furthermore, the hydrophilic surface of the LDH layers is incompatible with hydrophobic polymer molecules. For these two reasons, monomer and polymer molecules cannot easily penetrate into LDH layers nor can LDH layers be easily homogeneously dispersed in the hydrophobic polymer matrix. The pristine LDHs must be modified with suitable organic anions is required to eliminate these obstacles.

In fact, the intercalated LDHs/polymer nanocomposites associated with water-soluble polymers have been successfully prepared in several investigations using the following two methods [11–20]. The first method is the direct intercalation of polymeric anions into the LDH gallery during the co-precipitation or ion exchange process [11–13]. The second method is the intercalation of monomeric anions into the LDH gallery, followed by in situ polymerization [14–20]. Otherwise, using water insoluble polymers can be used to obtain intercalated LDHs/polymer nanocomposites [21]. Few reports are available on exfoliated LDHs/polymer nanocomposites in which the LDHs have a large high anion exchange capacity, which corresponds to the presence of layers that are tightly stacked by the attractive forces among the interlayer anions. This situation does not favor exfoliation. Restated, the use of LDHs to form exfoliated LDHs/polymer nanocomposites is difficult. Recently, Qu et al. successfully synthesized exfoliated LDHs/PE-*g*-MA [22] and LDHs/LLDPE [23] nanocomposites by refluxing in a non-polar xylene solution of PE-*g*-MA and LLDPE, respectively. In the author's laboratory, exfoliated LDHs/polyimide [24] and the LDHs/epoxy [25] nanocomposites were also fabricated by in situ condensation polymerization. The morphology of the exfoliated LDHs/polyimide and LDHs/epoxy nanocomposites is such that the LDH layers, which are homogeneously dispersed in the polymer matrix retained the ordered orientation. However, well exfoliated LDHs/poly(methyl methacrylate) has never before been investigated. Therefore, this study presents new experimental results that reveal that the exfoliated LDHs/poly(methyl methacrylate) nanocomposite with disordered LDH layers were successfully synthesized by a two-stage process with an in situ bulk polymerization, which consists methyl methacrylate and organically modified LDHs. The LDH layers were individually and homogeneously dispersed in the PMMA matrix.

2. Experimental details

2.1. Materials

The materials used in the synthesis of the 10-undecenoate intercalated layered double hydroxides, were $Mg(NO_3)_2\cdot 6H_2O$ (Fluka Co.), $Al(NO_3)_3\cdot 9H_2O$ (Fluka Co.), sodium hydroxide (Fluka Co.), sodium carbonate (Aldrich Co.) and 10-undecenoic acid (Fluka Co.). These were analytical reagent grade and used without further purification. The solvent used in the preparation of the LDHs was doubly deionized water whose conductivity was less than 0.4 μS/cm and whose pH was approximately 6.47 at room temperature. Methyl methacrylate (MMA) (Aldrich Co.) and 2,2′-azobisisobutyronitrile (AIBN) (Fluka Co.) were used to prepare the pristine PMMA resin and the exfoliated LDHs/PMMA nanocomposite. MMA monomer was twice purified by distillation under reduced pressure before it was used.

2.2. Preparation of Mg/Al LDH 10-undecenoate (LDH-U)

The Mg/Al LDH 10-undecenoate was synthesized by adopting the co-precipitation method. The preparation was performed in an N_2 atmosphere to exclude carbonate from the LDHs. NaOH (0.02 mol) was dissolved in 100 ml of doubly deionized water in a four-neck flask, and then, 10-undecenoic acid (0.02 mol) was added to the sodium hydroxide solution. Magnesium nitrate (0.02 mol) and aluminum nitrate (0.01 mol) were dissolved in 50 ml of doubly deionized water. The nitrate solution was then slowly dropped into the vigorously stirred 10-undecenoate/NaOH solution at room temperature. The pH of the solution was maintained at 10 by adding 1 M NaOH solution. After the nitrate solution had been added, the resulting precipitate was aged at 40 °C for 16 h, and was then filtered until all of the supernatant liquid was removed. The sample was washed several times by doubly deionized water and dried at 40 °C in a vacuum oven before it was used. LDH- CO_3^{2-} was prepared according to the co-precipitation method of Carlino et al. [26].

2.3. Preparation of LDHs/PMMA nanocomposite

The LDHs/PMMA nanocomposite was prepared by a two-stage process with in situ bulk polymerization. The experimental conditions were as follows. The first stage, pre-polymerization, in a 500 ml Pyrex reactor with inlets of mechanical stirring, refrigeration, and nitrogen, was placed LDH-U (10 g) and MMA (190 g). The mixture was stirred mechanically under nitrogen purging at room temperature

until the homogeneous mixture was formed. In this case, stirring for a few minutes dramatically increased the viscosity of the mixture producing a gel. Then, the mixture was held at 50 °C and AIBN (0.2 g) was added to pre-polymerize it. At appropriate time intervals, small amounts of polymer were taken and precipitated by adding methanol in excess by a factor of 20. The precipitated material was filtered and dried at 30 °C in a vacuum oven to calculate the conversion of MMA. The viscous mixture was cooled until a critical viscosity was reached, corresponding to the pre-polymerization of MMA.

In the second stage—casting polymerization—AIBN (0.2 g) was added again to the viscous mixture at room temperature, and then, the mixture was injected into the glass mold at 60 °C isothermal for 4 h. The glass mold was kept in an oven at 120 °C for 1 h to ensure that the polymerization of the MMA was complete. Finally, the glass mold was slowly cooled to room temperature and then the glass mold was removed to yield a transparent sheet of LDHs/PMMA nanocomposite.

2.4. Characterizations and measurements

The X-ray diffraction (XRD) patterns were determined using a Rigaku RINT2000 X-ray diffractometer, using Cu K_α radiation, at $2\theta = 0.05\ s^{-1}$ between 2 and 70°. The generator tension was 40 kV and the generator current was 30 mA. FT-IR analyses were performed using a Bio-Rad FTS-40A FT-IR analyzer. Spectra were obtained using a resolution of 4 cm^{-1}, averaged over 64 scans. KBr was used as a background material and disks of samples/KBr mixtures were prepared to obtain the FT-IR spectra. Carbon, hydrogen and nitrogen were analyzed using a Heraeus CHN-O-RAPID elemental analyzer (EA). Magnesium and aluminum were analyzed using a HEWLETT PACKARD 4500 inductively coupled plasma-mass (ICP) spectrometer. The solid-state ^{27}Al and ^{13}C magic angle spinning (^{27}Al and ^{13}C MAS NMR) spectrum was recorded with a Bruker AVANCE-400 solid-state NMR spectrometer. Transmission electron microscope (TEM) samples were cut using a Leica UCT Microtome with a diamond knife. Samples were collected on hexagonal 300 mesh copper grids. Micrographs were obtained using Hitachi HF-2000 FE TEM at an accelerating voltage of 200 kV.

3. Results and discussion

3.1. Characterization of LDH-U

The organically modified process plays an important role in the preparation of the exfoliated LDHs/PMMA nanocomposite. Therefore, the first purpose of this work is to synthesize suitable organo-LDHs for preparing the exfoliated LDHs/PMMA nanocomposite. The most effective method for achieving the objective is to use LDHs onto whose surface was a polymerizable anion with good affinity for MMA monomer. Therefore, the surface of the LDHs was modified using the 10-undecenoate as the organically modified agent, which contained a polymerizable end group [27].

Fig. 1 presents the XRD patterns of the LDH- CO_3^{2-} and the LDH-U. The XRD pattern of the LDH-U demonstrates that the strongest diffraction peak appeared at $2\theta = 2.9°$. The result reveals that the maximum observed basal spacing was 23.3 Å, corresponding to the interlayer spacing of 18.5 Å. The basal spacing of the LDH-U was increased because the volume of the 10-undecenoate anion is large. This finding reveals that 10-undecenoate anions had intercalated into the gallery of the LDH layers as confirmed by FT-IR, and presented in a forthcoming section. Additionally, Fig. 1(b) presents the diffraction peaks of (006) and (009), indicating that the layer characteristic of the LDH-U is extremely pronounced. Furthermore, the XRD pattern of LDH-U exhibits a sharp (003) diffraction peak whose reflection is indicative of long-range ordering in the stacking dimension. The coherence length in the stacking direction of the LDH-U is calculated by the Scherrer equation, $D_{hkl} = 0.9\lambda/\beta_{1/2}\cos\theta$, in which λ is the X-ray wavelength, θ the diffraction angle, and $\beta_{1/2}$ the width at half-maximum intensity [16]. The domain size of the LDH-U was found to be 20.3 nm, corresponding to about eight or nine stacked layers.

The structure of the LDH-U may contain a phase that corresponds to a monolayer of 10-undecenoate anions in the gallery of the LDH layers. A possible structure for the arrangement of 10-undecenoate anions within the inter-sheet galleries is proposed in Scheme 1; the carbon chains of the 10-undecenoate are tilted angle to the surface of LDH layers. A similar model of the monolayer structure of intercalated anions in the interlayer region of the LDH has been reported [28,29].

Fig. 2 shows the FT-IR spectra of the LDH- CO_3^{2-} and the LDH-U. A strong peak at 1365 cm^{-1} (Fig. 2(a)) is associated with the asymmetric stretching vibration of the carbonate anions [30,31]. The fingerprint peak at 610 cm^{-1} and that at 428 cm^{-1} are associated with M–O stretching modes in the LDH sheets [11]. The FT-IR spectrum of the LDH-U contains strong absorption peaks at 1559 and 1456 cm^{-1} that are assigned to the asymmetric and symmetric stretching vibrations, respectively, of $RCOO^-$. The characteristic peak associated with the C=C stretching vibration occurs at 1642 cm^{-1} while the peak at 3081 cm^{-1} corresponds to the C–H stretching vibration for the sp^2 carbon of the 10-undecenoate anion [32]. Fig. 2(b) also reveals that the peak at 1415 cm^{-1} is the scissoring bending vibration of the C–H in-plane bonds and the other two strong bands at 911 and 993 cm^{-1} are the out-of-plane bending vibration of C–H, which bonds to the 10-undecenoate anion. These FT-IR assignments demonstrate that the 10-undecenoate anion is successfully intercalated into the gallery of the LDH. However, the strong and broad absorption peak with a higher wavenumber in both the

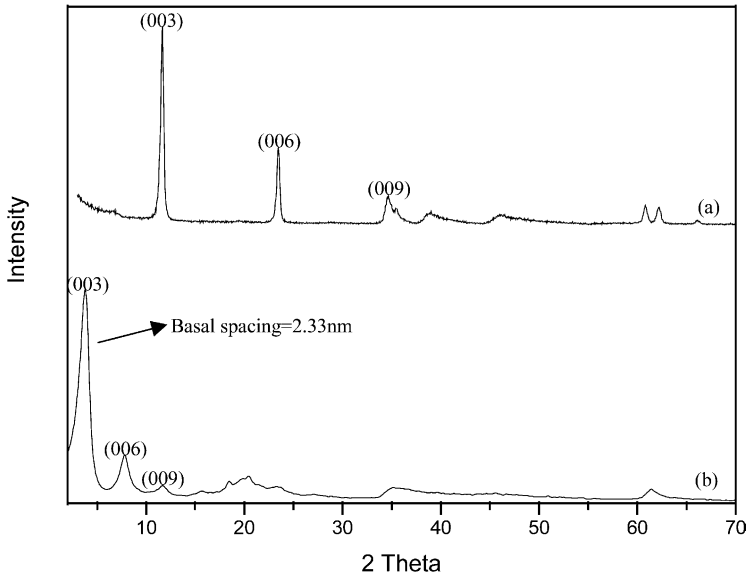

Fig. 1. XRD diffraction patterns of (a) LDH- CO_3^{2-} and (b) LDH-U.

FT-IR spectra of the LDH- CO_3^{2-} and that of the LDH-U is attributed to the –OH group in both the LDH sheets and the interlayer water molecules [33].

The ICP analysis of the LDH-U yielded the following results; Al, 2.59 ppm and Mg, 4.64 ppm. The C and H elemental analysis of the LDH-U yielded the following results; C, 31.46 wt% and H, 7.35 wt%. Nevertheless, the N elemental analysis of the LDH-U indicated that the N element content of the LDH-U is not observed. These experimental data suggest the following empirical formula.

$$Mg_{4.03}Al_2(OH)_{12.06}(CH_2 = CH(CH_2)_8COO^-)_{1.84}(CO_3^{2-})_{0.08}\cdot 6.28\ H_2O$$

Due to the solubility of magnesium hydroxide greatly exceeds that of aluminum hydroxide [34], the molar fraction of Mg^{2+}/Al^{3+} in LDH-U correlates perfectly with the molar fraction used in the recipe. However, the intercalary 10-undecenoate anion/Al^{3+} ratio in the LDH-U was 0.92, indicating that considerable quantities of the 10-undecenoate anions were intercalated into the gallery of the LDH layers and about 92% of the interlayer anions were exchanged by the 10-undecenoate anions. This result can be further proved by the ^{13}C MAS NMR spectra. In addition, the ^{27}Al MAS NMR spectrum of the LDH-U exhibits a single sharp resonance peak at +10.08 ppm. According to the literature [35,36], this result reveals that aluminum is coordinated in an octahedral geometry and the layered structure of the LDH-U is the same as that associated with the original brucite-like octahedral geometry, when the LDH-U is generated.

Fig. 3 displays the ^{13}C MAS NMR spectra of the sodium 10-undecenoate and the LDH-U. The resonance peaks observed on the spectrum of sodium 10-undecenoate are assigned according to the literature [32]. The spectrum of the LDH-U includes three principal resonance peaks are observed. The resonance peaks at 140.4 and 116.0 ppm are attributed to the carbon atoms of the vinyl group, C^b and C^a, respectively. The resonance peak occurs at 185.0 ppm is associated with the carboxylic group and the peaks between 27 and 40 ppm refer to the methylene carbons in the 10-undecenoate anion skeleton. However, according to the literature, the resonance peak at 170.6 ppm, associated with the interlayer charge balancing carbonate anion of the LDH, disappears [26]. Restated, the interlayer region of the LDH sheets contains considerable quantities of 10-undecenoate anions. On the other hands, for the LDH-U, the resonance peak of C_k is slightly shifted from the initial position for sodium 10-undecenoate to a downfield value. The shifts may be explained by a strong electrostatic interaction between the carboxylic group and the inner surface of the LDH that occurs when the 10-undecenoate anion is incorporated into LDH layers. Similar results have been observed for other intercalating anions in the LDHs [14,15,19,20].

Fig. 4 presents a typical TEM image of the LDH-U; the domain size of the LDH-U is seen clearly. The LDH-U with a stack of eight or nine layers has a regular basal spacing, which is close to the value determined by XRD. However, the domain size of the LDH-U also agrees with the result estimated from the XRD pattern using the Scherrer equation, as described above.

To sum up, all of the above evidence supports the fact that 10-undecenoate anions were successfully intercalated into the host LDH using the co-precipitation method.

3.2. Pre-exfoliate the stacked LDH-U during the pre-polymerization

In this study, a two-stage process that involves, pre-polymerization and in situ bulk polymerization, was used to

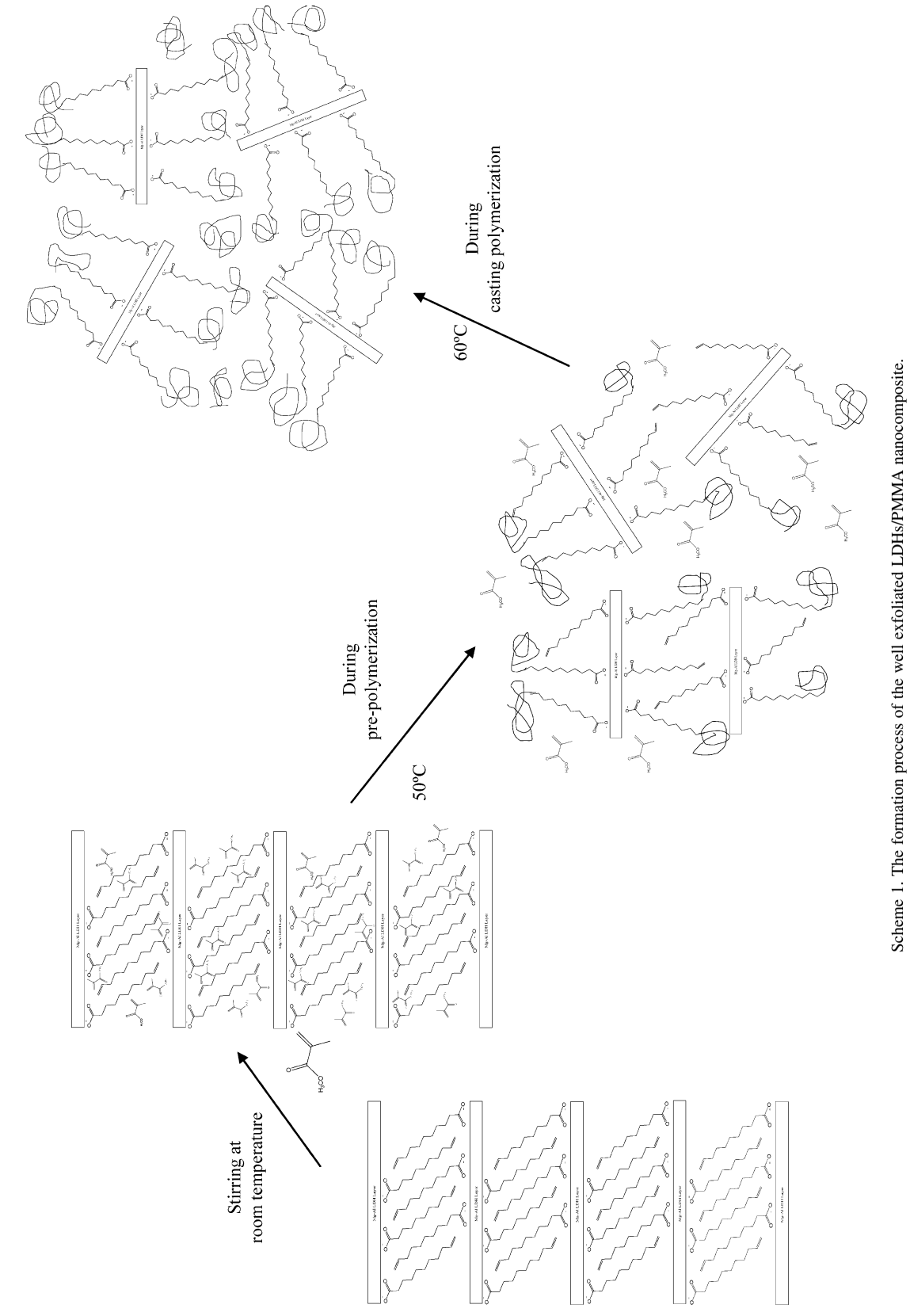

Scheme 1. The formation process of the well exfoliated LDHs/PMMA nanocomposite.

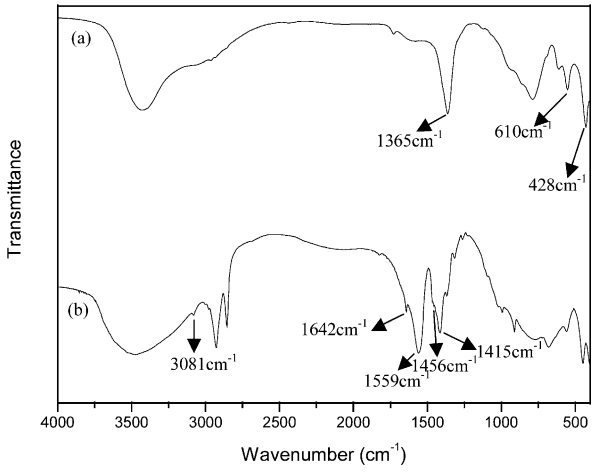

Fig. 2. FT-IR spectra of (a) LDH- CO_3^{2-}, (b) LDH-U.

yield a well exfoliated LDHs/PMMA nanocomposite. The pre-polymerization process was performed by heating the mixture of the LDH-U and the MMA at a low temperature. A decrease in the rate of decomposition of the initiator can appropriately increase the time required to achieve a critical viscosity, corresponding to the pre-polymerization of the MMA [37]. The MMA can simultaneously facilitate diffusion into the interlayer galleries of the LDH-U and increase the probability of the polymerization of MMA with the polymerizable 10-undecenoate anion of the LDH galleries.

Fig. 5(b)–(j) shows the XRD patterns of the product containing 5 wt% LDH-U at various conversions during the pre-polymerization process. The (003) diffraction peak in Fig. 5(b) is almost the same as the one associated with pristine LDH-U, implying that the MMA molecules do not effectively swell the LDH-U galleries during the stirring of the mixture at room temperature for 4 h. The conversion of the MMA monomer was zero at the mixing stage at room temperature, so the LDH-U lacked a kinetic driving force for parting the LDH layers. After stirring the mixture at room temperature for 4 h, the mixture held isothermally at 50 °C using a water bath and then AIBN was added to pre-polymerize the mixture. Notably, when the conversion of the MMA pre-polymerization was 6.3 wt%, as shown in Fig. 5(c), the (003) diffraction peak was at $2\theta = 3.6°$, indicating that the basal spacing of the LDH-U had slightly increased. Subsequently, the ordered layered structure of the LDH-U starts to become loose, enabling part of the PMMA to subsist in the LDH-U interlayer galleries [38]. However, the (003) diffraction peak further shifts toward a lower angle and become broad, as the conversion of the MMA pre-polymerization increases to 8.4 wt%. The experimental data in Fig. 5(d) reveal that the basal spacing of the LDH-U could be further increased and the stacked LDH-U has a looser lamellar structure. When the conversion of the MMA pre-polymerization exceeded 8.4 wt%, as shown in Fig. 5(d)–(i), the position of the (003) diffraction peak remained almost constant at $2\theta = 3.1°$, whereas the broadness of the (003) diffraction peak gradually increased to a large degree. In the XRD patterns, the width of the (003) diffraction peak for the stacked lamellar LDH-U is related to the domain size of the LDH-U layers. These results prove that the domain size of the LDH-U with a constant basal spacing became small because of local disorder in the LDH layer within LDH-U crystallites, as the conversion of the MMA pre-polymerization increased from 8.4 to 18.6 wt% [39]. After the pre-polymerization was terminated, no peak was observed in the measured range, as depicted in Fig. 5(j). This finding demonstrates that the stocked LDH-U layers were completely delaminated and homogeneously dispersed within the PMMA matrix [40].

From the XRD patterns, the experimental results can be interpreted as follows. The polymerization of the MMA that had diffused into the galleries of the LDH-U provided the kinetic driving force for the separation of LDH layers [39]. Therefore, the basal spacing of the LDH-U increases significantly as a function with the conversion of MMA, up to a constant value of about 2.85 nm. The conversion of MMA pre-polymerization further increases, the kinetic driving force of the separation of the LDH layers reduces the number of stacked layers. Finally, the polymer chains of PMMA destroy most of the attraction between each pair of layers, an exfoliated LDH layer is obtained.

Moreover, TEM is also used to elucidate the dispersal behavior of the LDH layers in the PMMA matrix. Fig. 6(a) and (b) display TEM images of the pre-polymerization product at low and high magnifications, respectively. The dark strips in the figures correspond to LDH layers that are perpendicular to the surface of sample. The TEM images show that the LDH layers are well dispersed in the PMMA and much less strongly oriented. Furthermore, the TEM image of exfoliated LDH layers in Fig. 6(b) also shows few small aggregates of LDH layers with substantial layer separation, in strong contrast to the pristine LDH-U with orderly stacked LDH layers as depicted in Fig. 4. These facts may explain why the peak in the XRD pattern for the pre-polymerization product, even at the LDH-U of 21.5 wt% remains absent. The results demonstrate that, in this case, the LDH layers lost their ordered stacking-structure, and were exfoliated in the PMMA matrix. Notably, the LDH layers remained able to be dispersed homogeneously in the PMMA matrix at a high LDH-U content (21.5 wt%), as calculated from the MMA conversion of 19.2 wt% after pre-polymerization.

In summary, in this study, the pre-exfoliate LDH-U layers that thoroughly disperse into the PMMA matrix has formed in the course of pre-polymerization at 50 °C.

3.3. The exfoliated LDHs/PMMA nanocomposites

As expected, after casting polymerization, the XRD pattern of the LDHs/PMMA nanocomposite as shown in

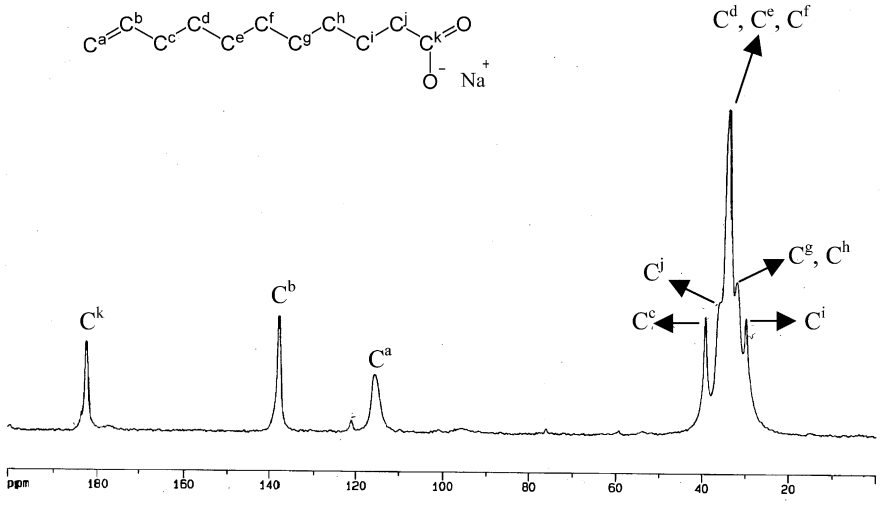

(a)

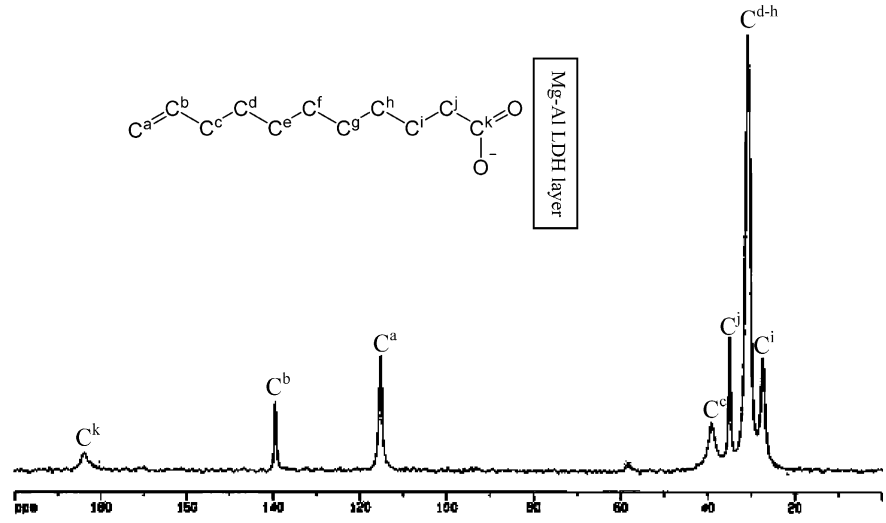

(b)

Fig. 3. ^{13}C MAS NMR spectra of (a) sodium 10-undecenoate and (b) LDH-U.

Fig. 5(k), do not include any diffraction peak as well as in Fig. 5(j), which indicates that the LDH layers were thoroughly exfoliated in the LDHs/PMMA nanocomposite. The TEM images in Fig. 7 also clearly show that the LDH layers were completely exfoliated and randomly dispersed in the PMMA matrix.

Moreover, both the pristine PMMA and the LDHs/PMMA nanocomposite were extracted with the acetone by the soxhlet equipment. Pristine PMMA was completely removed by acetone extraction without generating insoluble material. In contrast, for the LDHs/PMMA nanocomposite, the insoluble materials consisted of the LDH-U and the non-extracted PMMA that was attached to the LDH surface. The quantity of the recovered PMMA was approximately 79.2 wt% in the insoluble materials. This result indicates that the LDH layer surface interacts strongly with the residual PMMA. This interaction is attributable to the fact that polymerization occurs through MMA with the 10-undecenoate anion bound to the LDH layer surface, as also verified by FT-IR, as discussed in a forthcoming section. Wilkie et al. obtained a similar result while preparing montmorillonite/PMMA nanocomposites using

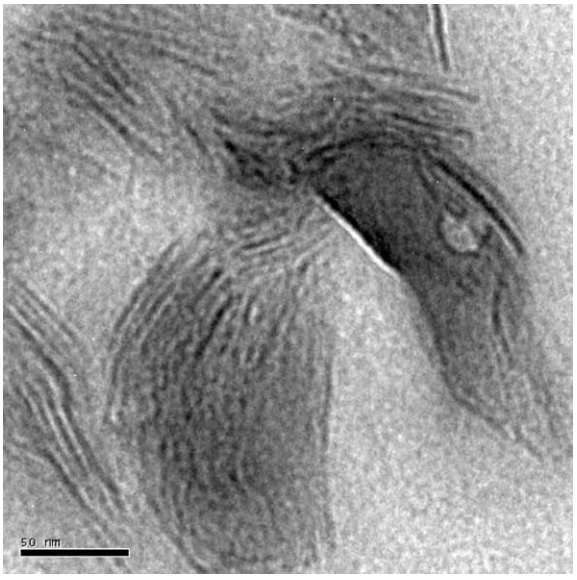

Fig. 4. TEM image of the LDH-U.

a surfactant that contained a styryl group [41]. However, the insoluble material was characterized by using FT-IR as showing in Fig. 8. The FT-IR spectrum of the insoluble material presents the characteristic peaks of both the LDH-U and the PMMA. Indeed, the absorption peaks of the C=O stretching vibration at 1730 cm^{-1} and the C–O stretching vibration at 1147 cm^{-1} confirm the presence of the PMMA [38]. Additionally, the M–O stretching vibrations at 610 and 428 cm^{-1}, the COO^{-} stretching vibrations at 1559 and 1456 cm^{-1} and the O–H stretching vibration between 3000 and 3700 cm^{-1} reveal the characteristic peaks from LDH-U. Notably, the disappearance of the absorption peak at 1640 cm^{-1} associated with the C=C stretching of the

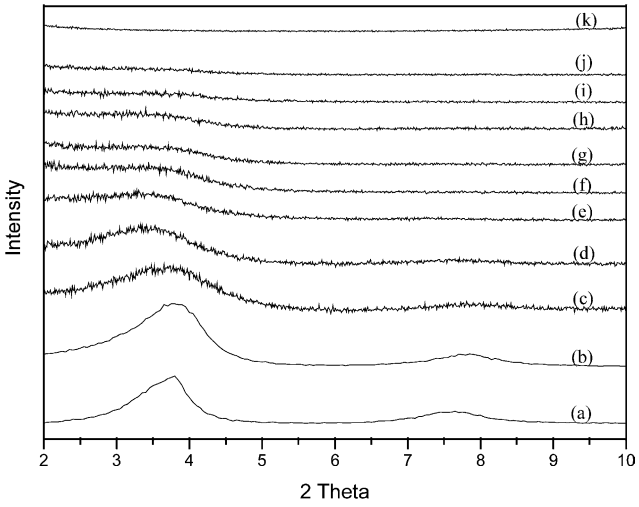

Fig. 5. XRD diffraction patterns of the product obtained at various conversions of MMA during the pre-polymerization process (a) pristine LDH-U, (b) mixture stirring at room temperature, (c) 6.3 wt%, (d) 8.4 wt%, (e) 10.5 wt%, (f) 13.2 wt%, (g) 16.2 wt%, (h) 17.1 wt%, (i) 18.3 wt%, (j) 19.6 wt%, and (k) LDHs/PMMA nanocomposite.

(a)

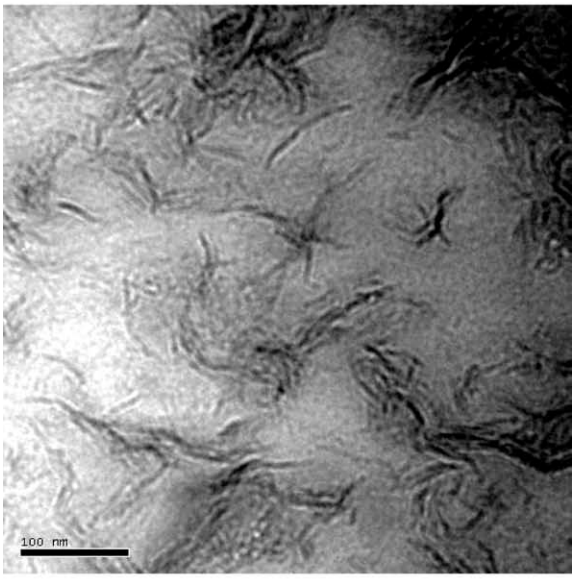

(b)

Fig. 6. TEM images of the pre-polymerization product at (a) low magnification and (b) high magnification.

10-undecenoate anion indicates that the polymerization occurred on the 10-undecenoate anion bound to the LDH layer surface. Consequently, all experimental findings support the claim that well exfoliated LDHs/PMMA nanocomposite had been prepared successfully.

4. Conclusions

10-Undecenoate can be intercalated into the interlayers of LDH layers by the co-precipitation method, and exfoliated LDHs/PMMA nanocomposite was successfully synthesized by a two-stage in situ bulk polymerization.

(a)

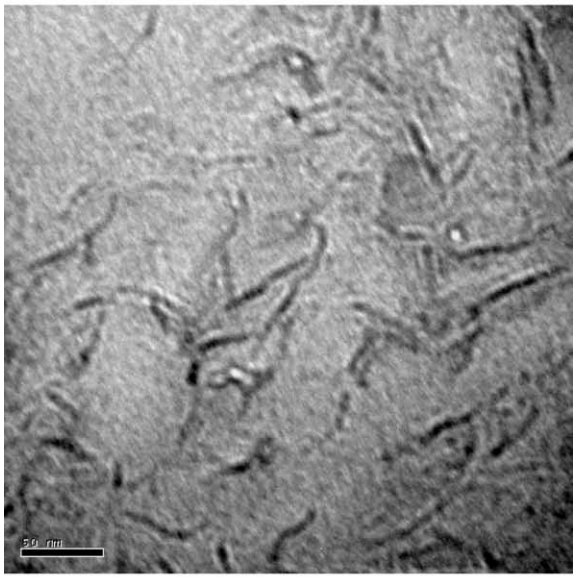

(b)

Fig. 7. TEM images of the exfoliated LDHs/PMMA nanocomposite at (a) low magnification and (b) high magnification.

Notably, the LDH layers could be well dispersed in the PMMA matrix at high LDH-U content (21.5 wt%) for the pre-polymerization product. The TEM result shows that the exfoliated LDH layers were dispersed in a disorderly manner in the PMMA matrix. Polymerization occurred on the 10-undecenoate anion bound to the LDH layer surface, as proven by FT-IR, so exfoliated LDHs/PMMA nanocomposite with disordered LDH layers is formed.

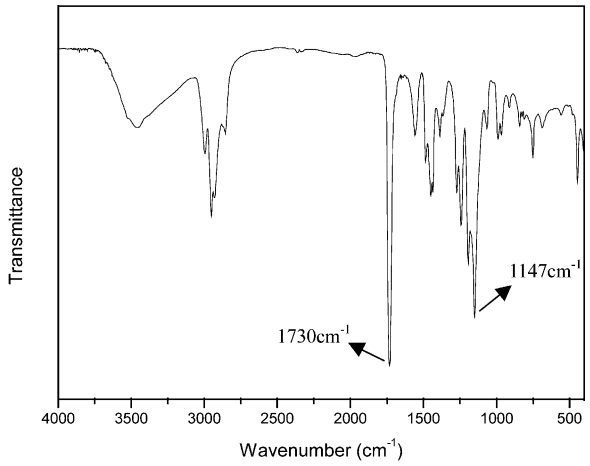

Fig. 8. FT-IR spectrum of insoluble material after extraction with the acetone in the LDHs/PMMA nanocomposite.

Acknowledgements

The authors thank the Ministry of Economic Affairs of the Republic of China for financially supporting this research under Contract No. TDPA: 92-EC-17-A-05-S1-0014.

References

[1] Robello DR, Yamaguchi N, Blanton T, Bames C. J Am Chem Soc 2004;126:8118.
[2] Gilman JW, Jackson CL, Morgan AB, Harris R. Chem Mater 2000;12:1866.
[3] Kim YK, Choi YS, Wang KH, Chung IJ. Chem Mater 2002;14:4990.
[4] Fu X, Qutubuddin S. Polymer 2001;42:807.
[5] Tripathy AR, Burgaz E, Kukureka SN, MacKnight WJ. Macromolecules 2003;36:8593.
[6] Constantino VRL, Pinnavaia TJ. Inorg Chem 1995;34:883.
[7] Iyi N, Kurashima K, Fujita T. Chem Mater 2002;14:583.
[8] Hibino T. Chem Mater 2004;16:5482.
[9] Xu ZP, Braterman PS, Yu K, Xu H, Wang Y, Brinker CJ. Chem Mater 2004;16:2750.
[10] Dimotakis ED, Pinnavaia TJ. Inorg Chem 1990;29:2393.
[11] Oriakhi CO, Farr IV, Lerner MM. J Mater Chem 1996;6:103.
[12] Lin JJ, Juang TY. Polymer 2004;45:7887.
[13] Liao CS, Ye WB. Electrochim Acta 2004;49:4993.
[14] Vieille L, Taviot-Gueho C, Besse JP, Leroux F. Chem Mater 2003;15:4369.
[15] Roland-Swanson C, Besse JP, Leroux F. Chem Mater 2004;16:5512.
[16] Moujahid EM, Dubois M, Besse JP, Leroux F. Chem Mater 2002;14:3799.
[17] Vaysse C, Guerlou-Demourgues L, Delmas C, Duguet E. Macromolecules 2004;37:45.
[18] Vaysse C, Guerlou-Demourgues L, Duguet E, Delmas C. Inorg Chem 2003;42:4559.
[19] Moujahid EM, Inacio J, Besse JP, Leroux F. Microporous Mesoporous Mater 2003;57:37.
[20] Moujahid EM, Besse JP, Leroux F. J Mater Chem 2002;12:3324.
[21] Challier T, Slade RCT. J Mater Chem 1994;4:367.
[22] Chen W, Qu B. Chem Mater 2003;15:3208.
[23] Chen W, Feng L, Qu B. Chem Mater 2004;16:368.
[24] Hsueh HB, Chen CY. Polymer 2003;44:1151.
[25] Hsueh HB, Chen CY. Polymer 2003;44:5275.
[26] Carlino S, Hudson MJ. J Mater Chem 1994;4:99.
[27] Friberg S, Thundathil R, Stoffer J. Science 1979;205:607.
[28] Kanoh T, Shichi T, Takagi K. Chem Lett 1999;28:117.

[29] Costantino U, Marmottini M, Nocchetti M, Vivani R. Eur J Inorg Chem 1998;10:1439.
[30] Miyata S. Clays Clay Miner 1975;23:369.
[31] Iyi N, Matsumoto T, Kaneko Y, Kitamura K. Chem Mater 2004;16: 2926.
[32] McGrath KM. Colloid Polym Sci 1996;274:499.
[33] Taibi M, Ammar S, Jouini N, Fiévet F, Molinié P, Drillon M. J Mater Chem 2002;12:3238.
[34] Costantino U, Marmottini F, Nocchetti M, Vivani R. Eur J Inorg Chem 1998;10:1439.
[35] Reichle WT. J Catal 1985;94:547.
[36] Carlino S, Hudson MJ, Husain SW, Knowles JA. Solid State Ionics 1996;84:117.
[37] Avella M, Emanuela E, Martuscelli E. Nano Lett 2001;1:213.
[38] Choi YS, Choi MH, Wang KH, Kim SO, Kim YK, Chung IJ. Macromolecules 2001;34:8978.
[39] Zeng C, Lee LJ. Macromolecules 2001;34:4098.
[40] Yeh JM, Liou SJ, Lin CY, Cheng CY, Chang YW, Lee KR. Chem Mater 2002;14:154.
[41] Su S, Wilkie CA. J Polym Sci, Polym Chem 2003;41:1124.